Thermal Decomposition of some Alkali-metal Oxalate Monohydrates and Monoperhydrates †

By **John M. Adams** * and **Vijayalakshmi Ramdas**, Edward Davies Chemical Laboratories, University College of Wales, Aberystwyth, Dyfed SY23 1NE
Giulio G. T. Guarini, Institute of Physical Chemistry, University of Florence, Florence, Italy
Christopher J. Adams, Unilever Research Laboratory, Port Sunlight, Wirral, Merseyside L62 4XN

The kinetics of the decomposition of a series of alkali-metal oxalate perhydrates and their related hydrates have been studied by a combination of thermogravimetric analysis, differential scanning calorimetry, and optical microscopy. The behaviour of the perhydrates is strikingly similar to that of the related hydrate (where this exists). The kinetic formulations which best fit the decompositions have been ascribed and activation energies obtained for experiments carried out in a static atmosphere (E_a = 64—208 kJ mol^{-1} for perhydrates, 98—250 kJ mol^{-1} for hydrates).

PERHYDRATES are of considerable technical importance as carriers of hydrogen peroxide. However, all known perhydrates are more or less unstable. Decomposition is continuous under typical laboratory conditions, where the time for complete loss of peroxide ranges from a few hours to several months. Typically, the rate of decomposition at room temperature is a function of relative humidity.[1]

The structures of perhydrates are akin to those of hydrates: hydrogen bonds hold the H_2O_2 molecules in the lattice. The thermal decompositions of the two classes of compound also show similar features: heating perhydrates releases H_2O_2 into the atmosphere,[1] just as the dehydration of hydrates releases water. However, while the kinetics of dehydration reactions have been reported for a number of hydrates,[2] no thorough investigation has been made of the deperhydration of perhydrates.

We report in this paper our attempt to establish the kinetics of decomposition of a series of oxalate perhydrates, $M_2[C_2O_4]\cdot H_2O_2$ (M = Li, Na, K, Rb, or NH_4), using thermogravimetric analysis (t.g.a.), differential scanning calorimetry (d.s.c.), and hot-stage optical microscopy.[2] These techniques were also applied to the dehydration of the hydrates $M_2[C_2O_4]\cdot H_2O$ (M = K, Rb, or NH_4) *which are isostructural with the corresponding perhydrates.*[3-9] Thus, we are able to present a direct comparison of the decomposition kinetics of hydrates and perhydrates. The decomposition products of the deperhydration reaction are H_2O_2 vapour [1] and anhydrous oxalate (determined by *X*-ray diffraction).

EXPERIMENTAL

Thermogravimetric Analysis.—A Stanton Redcroft TG770 instrument with aluminium sample holders was used throughout. For perhydrates the reaction kinetics were affected by the nature of the sample holder (*e.g.* whether or not it had been previously used, *etc.*) and so the same holder (which was cleaned and dried the same way for each experiment) was used for all runs. Polythermal and isothermal data were obtained, both in a static atmosphere (air) and a flowing dry nitrogen atmosphere.

Differential Scanning Calorimetry.—A Perkin-Elmer DSC-1b with aluminium sample holders was used with an empty pan for reference. For the hydrates the sample was covered with a thin layer of powdered graphite, as was the reference pan. This has been shown to improve the baseline by reducing the difference in thermal emissivity of the sample and the reference.[10] In the case of the perhydrates, however, graphite caused catalytic decomposition and hence loose aluminium lids had to be used. In all the runs care was taken to ensure that the sample was spread as a thin even layer, in the bottom of the pan, giving good contact; otherwise a single peak turned into incomplete multiple peaks.

Hot-stage Optical Microscopy.—The results obtained by the above techniques were supported by observations made of the thermal decomposition through a Reichert binocular microscope equipped with a hot stage and facilities for photography.

Sample Preparation.—Commercial samples of $K_2[C_2O_4]\cdot H_2O$ and $[NH_4]_2[C_2O_4]\cdot H_2O$ were recrystallised from aqueous solution. The compound $Rb_2[C_2O_4]\cdot H_2O$ was prepared from the carbonate by treatment with calculated quantities of oxalic acid dihydrate, and was subsequently recrystallised. The perhydrates were prepared by the recrystallisation of corresponding oxalates from 50% H_2O_2.

Conditions.—The nature of perhydrate decompositions restricts the choice of experimental conditions, as follows. (*i*) Crystalline powders were used, since single perhydrate crystals tend to shatter explosively on heating. A particle size <63 μm was achieved by grinding the recrystallised solid samples and then passing them through an ASTM No. 240 mesh. (*ii*) Irreproducible results were obtained when a flowing nitrogen atmosphere was used for the perhydrate decomposition. Hence the results quoted were obtained with a static atmosphere. (*iii*) The optimum sample mass was *ca.* 4 mg. Larger samples gave irreproducible results, especially for the perhydrates.[11]

As far as possible the hydrates and perhydrates were examined under identical conditions, to ensure that a valid comparison of the kinetics could be made.

RESULTS AND DISCUSSION

The results of the investigations are summarised in the Table. Evidence for a particular kinetic law was obtained by plotting f(α) against t [where f(α) is a function of α (extent of reaction) appropriate to the law under examination, and t is the time] for the various possible models, and adopting the model which best fits the results.[12] Once the kinetic equation followed by the reaction has been established over a reasonable range of

---

† The monoperhydrates are hydrogen peroxide (1/1) adducts.

α, an overall activation energy for the reaction can be obtained from the Arrhenius equation.[13] In particular, experimental results from isothermal decompositions were tested against four models: (*i*) power law, $\alpha = kt^n$; (*ii*) contracting circle, $1 - (1 - \alpha)^{\frac{1}{2}} = kt$; (*iii*) contracting sphere, $1 - (1 - \alpha)^{\frac{1}{3}} = kt$; and (*iv*) Avrami–Eroveef, $-\ln(1 - \alpha) = kt^n$. Plots of α/t against t for each of these theoretical curves are shown in Figure 1, as these are known to be useful in distinguishing different kinetic behaviour.[14]

Summary of results

Salt	Atmosphere	Temperature at which reaction starts (T/K)	ΔH/kJ mol^{-1}	Kinetic law	E/kJ mol^{-1}
$K_2[C_2O_4]\cdot H_2O$	Static air	340	59 ± 3	Avrami–Eroveef ($n = 2$)	198
	Flowing nitrogen [14]	330		Avrami–Eroveef ($n = 2$)	
$K_2[C_2O_4]\cdot H_2O_2$	Static air	400	-18.5 ± 1.5	($n = 1$) Power law or	208
				Avrami–Eroveef ($n = 2$)	166
$Rb_2[C_2O_4]\cdot H_2O$	Static air	355	60 ± 1	(Nucleation, possibly contracting circle or ‘ first-order ’ or ‘ exponential ’)	
				Avrami–Eroveef ($n = 2$)	247
	Flowing nitrogen 6.8 cm^3 min^{-1}	340	61 ± 2		
	28.5 cm^3 min^{-1}	340	62 ± 1		
$Rb_2[C_2O_4]\cdot H_2O_2$	Static air	415	-21 ± 2	(Nucleation, possibly contracting circle or ‘ first-order’ or ‘ exponential ’)	
				Avrami–Eroveef ($n = 2$)	159
$[NH_4]_2[C_2O_4]\cdot H_2O$	Static air	315	51 ± 2	(Nucleation, probably power law with $n > 2$) Contracting circle	98
	Flowing nitrogen 6.9 cm^3 min^{-1}	310	52 ± 2	(Nucleation, probably power law with $n > 2$) Contracting circle	93
	12.0 cm^3 min^{-1}		49 ± 1		(at flow rate 21 cm^3 min^{-1})
	16.6 cm^3 min^{-1}		50 ± 1		
	27.9 cm^3 min^{-1}		48 ± 2		
$[NH_4]_2[C_2O_4]\cdot H_2O_2$	Static air	(355—350)	>0		
$Na_2[C_2O_4]\cdot H_2O_2$	Static air	360	36.5 ± 7.5	($n = 1$) Power law	81
				or contracting circle	64

Hydrates.—For all the hydrates the temperature of decomposition proved to be a function of the atmosphere; loss of water occurred at lower temperatures in a flowing nitrogen atmosphere than in a static atmosphere. However, the enthalpy of reaction, ΔH (calculated from the area under the d.s.c. peak), did not vary with the experimental conditions. The presence of water vapour in the atmosphere thus affects the rate but not the thermodynamics of the reaction.

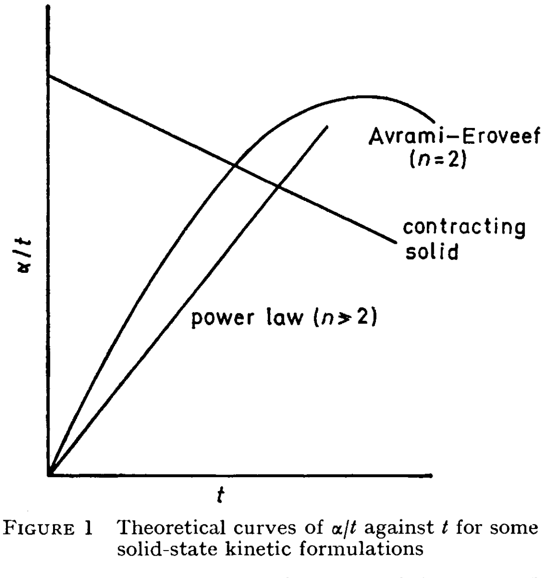

FIGURE 1 Theoretical curves of α/t against t for some solid-state kinetic formulations

$K_2[C_2O_4]\cdot H_2O$. Our results compare reasonably well with an earlier study of the dehydration of this compound.[15] Isothermal decomposition gave sigmoid t.g.a. curves with relatively short induction periods (Figure 2). Although the induction period varied considerably between different runs at one temperature, the decomposition curves subsequently became parallel. Plots of α/t against t give maxima at about $\alpha = 0.80$, suggesting that the Avrami–Eroveef law applies to the reaction [Figures 1 and 2(*b*)]; plots of $\ln[1/(1 - \alpha)]^{\frac{1}{2}}$ against t [Figure 2(*b*)] gave good straight lines at all temperatures studied, confirming that $n = 2$ for the Avrami–Eroveef equation. However, the value of the activation energy obtained from our Arrhenius plots was 198 kJ mol^{-1}, significantly higher than that given by the earlier work (70—140 kJ mol^{-1}), although it was reported that higher values were obtained in a static atmosphere.

The (001) face of a single crystal was observed during decomposition using the optical microscope. There was an initial formation of discrete nuclei. This stage was followed by rapid radial growth of the nuclei, leading eventually to overlap and to complete decomposition. These observations support the interpretation that the reactions follow Avrami–Eroveef kinetics.

$Rb_2[C_2O_4]\cdot H_2O$. The decomposition of the rubidium salt resembled that of the potassium one, but water loss occurs at a slightly higher temperature (355 and 340 K, in static air). Plots of α/t against t show maxima in the range $\alpha = 0.75$—0.90, suggesting the Avrami–Eroveef mechanism, while the linearity of the plot of $\ln[1/(1 - \alpha)]^{\frac{1}{2}}$ against t confirms that $n = 2$ (Figure 3). The activation energy, 247 kJ mol^{-1}, is rather high, presumably because of the static atmosphere.

Differences from $K_2[C_2O_4]\cdot H_2O$ are seen in the early part of the decomposition. Here the plot of α/t for $Rb_2[C_2O_4]\cdot H_2O$ has a negative slope, indicating that nucleation is a different kinetic process, and is not purely random throughout the solid (Figure 3). The slope of −1 might be consistent with a contracting envelope type of mechanism or by a 'first-order' or 'exponential' nucleation.[15] No attempt was made to measure the

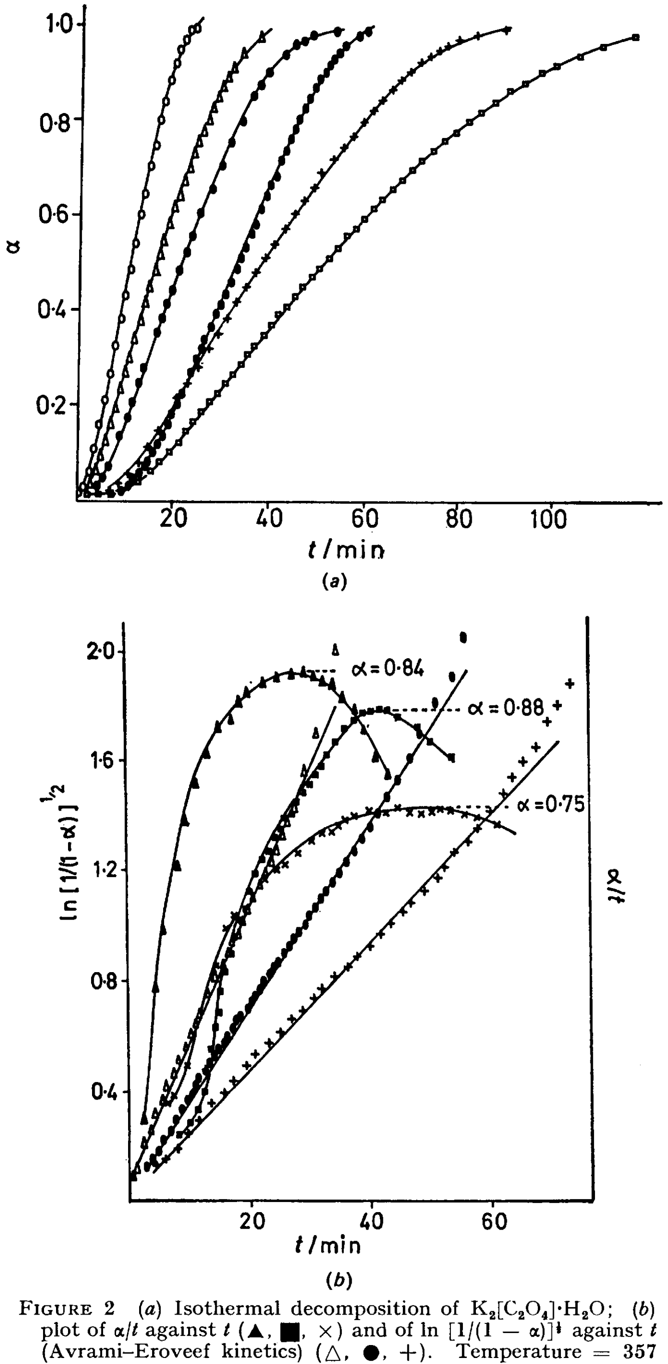

FIGURE 2 (a) Isothermal decomposition of $K_2[C_2O_4]\cdot H_2O$; (b) plot of α/t against t (▲, ■, ×) and of $\ln[1/(1-\alpha)]^{\frac{1}{2}}$ against t (Avrami–Eroveef kinetics) (△, ●, +). Temperature = 357 (○), 353 (△,▲), 352 (●,■), 349 (+,×), or 347 K (□)

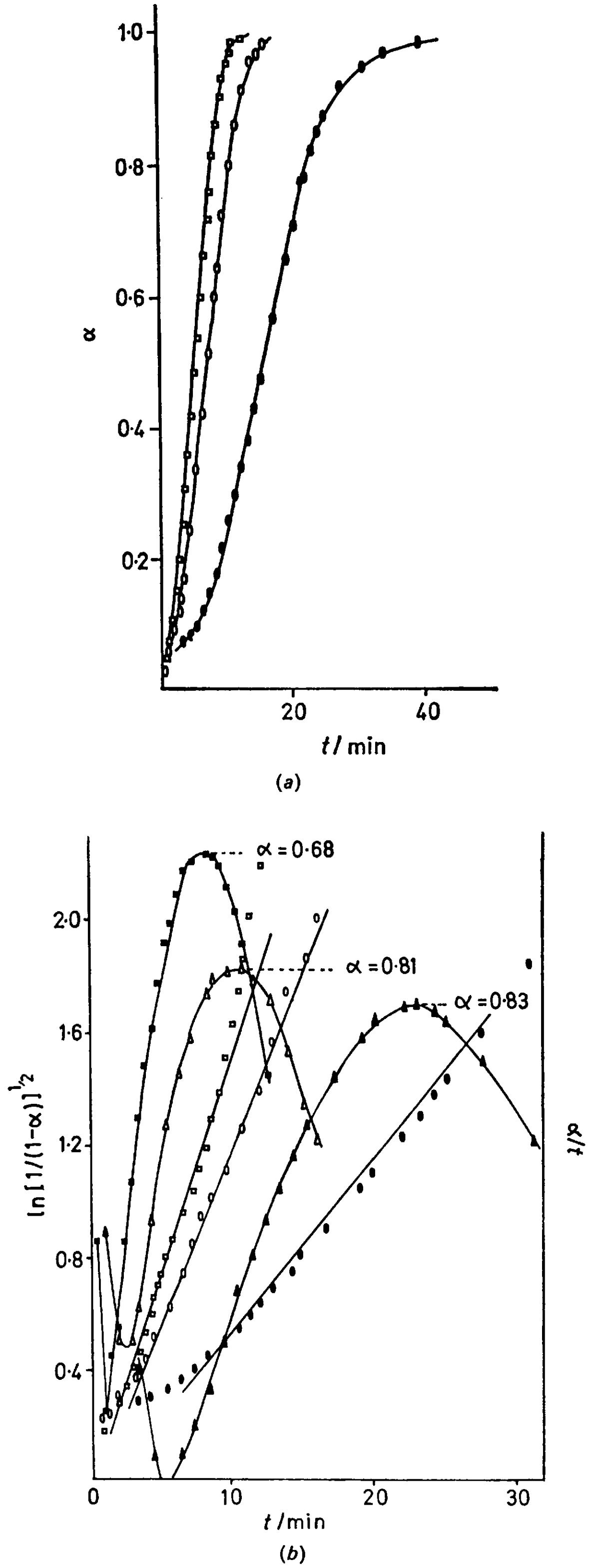

FIGURE 3 (a) Isothermal decomposition of $Rb_2[C_2O_4]\cdot H_2O$; (b) plot of α/t against t (■, △, ▲) and of $\ln[1/(1-\alpha)]^{\frac{1}{2}}$ against t (Avrami–Eroveef kinetics) (□, ○, ●). Temperature = 381 (□,■), 379.5 (○,△), or 376.5 K (●,▲)

activation energy, because of uncertainties in the temperature of the sample during the initial minute of the experiment. However, optical microscopic examination could not reveal any differences between the nucleation processes of $K_2[C_2O_4]\cdot H_2O$ and $Rb_2[C_2O_4]\cdot H_2O$.

$[NH_4]_2[C_2O_4]\cdot H_2O$. This hydrate loses its water at lower temperatures than either the potassium or the rubidium compound. Isothermal t.g.a. runs show a change of slope at $\alpha = 0.25$—0.30 (Figure 4), suggesting a change in the mode of decomposition; the derived plots of α/t against t show this effect very clearly. The latter part of the curve is consistent with a contracting circle type of equation for the decomposition kinetics. The nucleation, however, is not instantaneous (as is assumed in the derivation of the law) and possibly follows a power law, with $n = 2$ or more. Again no attempt has been made to calculate an activation energy for nucleation, because of temperature inaccuracies when t is small. For the main part of the reaction, the contracting circle seems to be followed both in air and in flowing nitrogen. The hydrate has a layered structure,[6] and so the contracting circle is more appropriate than the contracting sphere. Arrhenius plots give an activation energy of 98 kJ mol^{-1} in a static atmosphere: similar to those obtained in the dehydration of $BaCl_2\cdot 2H_2O$, which also follows a contracting circle equation.[11]

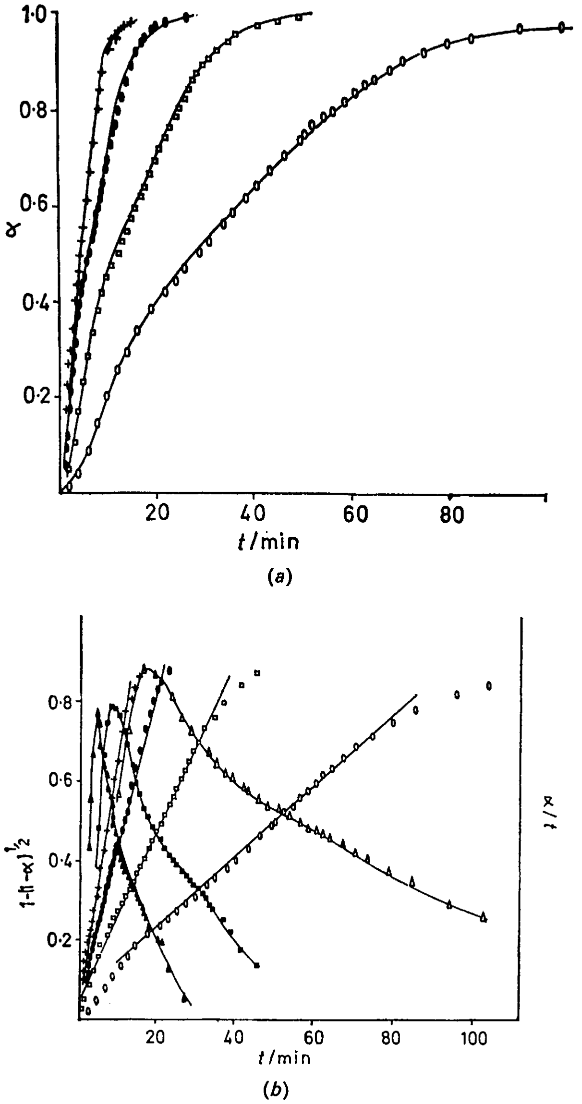

(a)

(b)

FIGURE 4 (a) Isothermal decomposition of $[NH_4]_2[C_2O_4]\cdot H_2O$ in static air; (b) plot of α/t against t for the decomposition in air (△, ■, △) and of $1 - (1 - \alpha)^{\frac{1}{2}}$ against t (contracting-circle kinetics) (+, ●, □, ○). Temperature = 335 (+), 329 (●, ▲), 324 (□, ■), or 318 K (○, △)

Perhydrates.—In previous studies perhydrates have been found to give d.s.c. traces which show a mixture of endothermic and exothermic effects, because two reactions are occurring [see equations (1) and (2)]. The

$$M\cdot H_2O_2(s) \longrightarrow M(s) + H_2O_2(g) \text{ Endothermic} \quad (1)$$

$$H_2O_2(g) \longrightarrow H_2O(g) + \tfrac{1}{2}O_2(g) \text{ Exothermic} \quad (2)$$

presence of hydrogen peroxide in the atmosphere over heated samples was shown by the yellow colour developed in test papers impregnated with potassium oxalatotitanate.[1] The d.s.c. results obtained in this work for the alkali-metal oxalate perhydrates are not typical of perhydrates generally.

$K_2[C_2O_4]\cdot H_2O_2$. Unusually for a perhydrate, this compound gave a single smooth exothermic peak, which was integrated to give a reproducible value of -18.5 ± 1.5 kJ mol^{-1} for the decomposition in a static atmosphere (Figure 5). Use of a flowing nitrogen atmosphere made the ΔH value irreproducible, and shifted the reaction to lower temperatures. However, the reaction still began at a higher temperature than that of the corresponding hydrate.

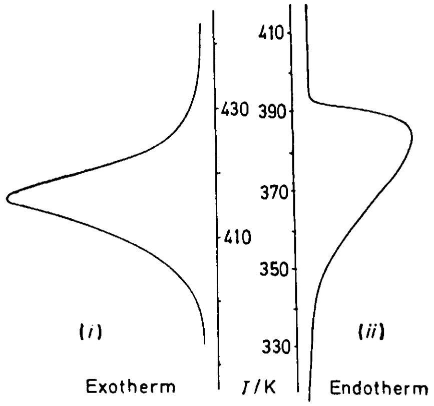

FIGURE 5 Differential scanning calorimetric runs on (i) $K_2[C_2O_4]\cdot H_2O_2$ and (ii) $K_2[C_2O_4]\cdot H_2O$. The rubidium oxalate perhydrate and hydrate behave in a very similar manner

The overall exothermic heat of the decomposition, ΔH, derives from two reactions, equations (3) and (4). Now

$$K_2[C_2O_4]\cdot H_2O_2(s) \longrightarrow K_2[C_2O_4](s) + H_2O_2(g) \quad \Delta H_1 \quad (3)$$

$$H_2O_2(g) \longrightarrow H_2O(g) + \tfrac{1}{2}O_2(g) \quad \Delta H_2 \quad (4)$$

$$\Delta H = \Delta H_1 + \Delta H_2 = -18.5 \text{ kJ mol}^{-1}$$

ΔH_2 is known to be -115 kJ mol^{-1},[16] and so $\Delta H_1 = 96.5 \pm 1.5$ kJ mol^{-1}. This represents the upper limit for the heat of the deperhydration reaction, since it assumes that all the H_2O_2 decomposes in the area of the sensors. That the measured ΔH varies for a flowing atmosphere is probably caused by the removal of various amounts of H_2O_2 before decomposition can occur.

T.g.a. plots of the isothermal decomposition of $K_2[C_2O_4]\cdot H_2O_2$ (at 368, 371, and 377 K) were linear over a very large range of α (0.05—0.90), but plots of α/t against t show maxima at α *ca.* 0.8 (Figure 6): the Avrami-Eroveef plot is linear up to α *ca.* 0.75. Activation energies for the reaction were calculated (*i*) from the linear t.g.a. plots (208 kJ mol^{-1}) and (*ii*) from the Avrami-Eroveef plots (166 kJ mol^{-1}). The reason for the discrepancy is not clear, but the observation of linear α/t t.g.a. isotherms is consistent with the propagation of chain reactions even within the subgrain boundaries.[17] Microscopic observation of the decomposition revealed random nucleation, followed by growth of individual nuclei. Photographs of the 001 face of a heated single crystal show changes similar to those observed for $K_2[C_2O_4]\cdot H_2O$.

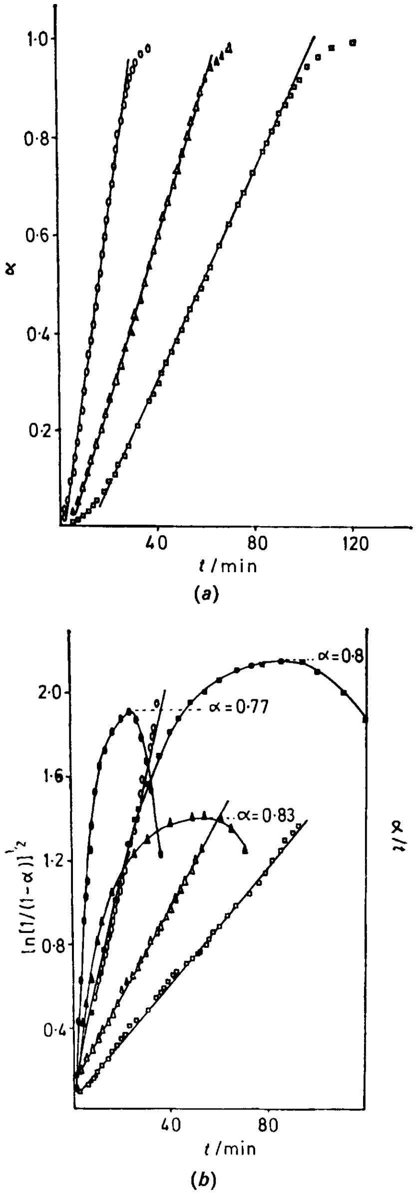

(*a*)

(*b*)

FIGURE 6 (*a*) Isothermal decomposition curve of $K_2[C_2O_4]\cdot H_2O_2$; (*b*) plot of α/t against t (■, ▲, ●) and of $\ln[1/(1-\alpha)]^{\frac{1}{2}}$ against t (Avrami–Eroveef kinetics) (□, △, ○). Temperature = 368 (□,■), 371 (△,▲), or 377 K (○,●)

$Rb_2[C_2O_4]\cdot H_2O_2$. Like $K_2[C_2O_4]\cdot H_2O_2$, the rubidium oxalate perhydrate gives a single smooth exotherm on d.s.c. investigation. The enthalpy of the decomposition (21 ± 2 kJ mol^{-1}) is very close to that of the potassium compound. Isothermal t.g.a. traces (at 386.5, 389, and 392 K) are typical sigmoid curves, and the derived plots of α/t against t show maxima at $\alpha = 0.75$ and a minimum at *ca.* 0.1 (Figure 7). Avrami-Eroveef plots are linear above $\alpha = 0.1$, and the activation energy was, at 159 kJ mol^{-1}, similar to that of the potassium compound. The negative slope of the α/t against t curves at small values of α parallels that of the hydrate. Again the nucleation period follows a different kinetic law from the bulk of the reaction.

$Na_2[C_2O_4]\cdot H_2O_2$ *and* $Li_2[C_2O_4]\cdot H_2O_2$. Both of these compounds are very unstable. The lithium salt perhydrate decomposes completely within a few hours of preparation. It also decomposes on being powdered. The sodium salt is slightly more stable, decomposing to the extent of 50% in *ca.* 24 h. However, it showed no tendency to decompose on being powdered. No kinetic studies have been made on the decomposition of the lithium compound.

Unlike the potassium and rubidium oxalate perhydrates, both of these compounds give single endothermic d.s.c. peaks with the decomposition temperatures being considerably lower than that of the potassium and rubidium samples. $Na_2[C_2O_4]\cdot H_2O_2$ is completely decomposed by 355 K and $Li_2[C_2O_4]\cdot H_2O_2$ at still lower temperatures. In the case of the lithium compound a reliable ΔH value could not be obtained due to the sample decomposition. With $Na_2[C_2O_4]\cdot H_2O_2$ the ΔH values varied between 29 and 44 kJ mol^{-1}. These values were too low to be the true heat of the deperhydration reaction, being much lower even than those given for the usual range of dehydration processes. This behaviour must again be due to some small amount of H_2O_2 vapour being catalytically decomposed upon the sample pan. Due to the lower decomposition temperature, a smaller proportion of the released H_2O_2 is decomposed than in the other cases, thus giving an overall endothermic effect.

Isothermal t.g.a. experiments were carried out at four different temperatures on the sodium oxalate perhydrate. The α against t curves were linear over the range $\alpha = 0.15$—0.70 [Figure 8(*a*)]. The slopes of the rectilinear portions of the curves used in an Arrhenius plot give an activation energy of 81 kJ mol^{-1}. However, the contracting circle equation [indicated by Figure 8(*b*)] gave good straight lines for $f(\alpha)$ against t curves [Figure 8(*b*)]. The Arrhenius plot made from these data gave an activation energy of 64 kJ mol^{-1}, which is in reasonable agreement with the value obtained from the

($n = 1$) power-law plots. It is therefore not possible to select which of the two kinetic laws best represents this decomposition. This situation has been met before and the selection of the more probable mechanism is extremely difficult.[11]

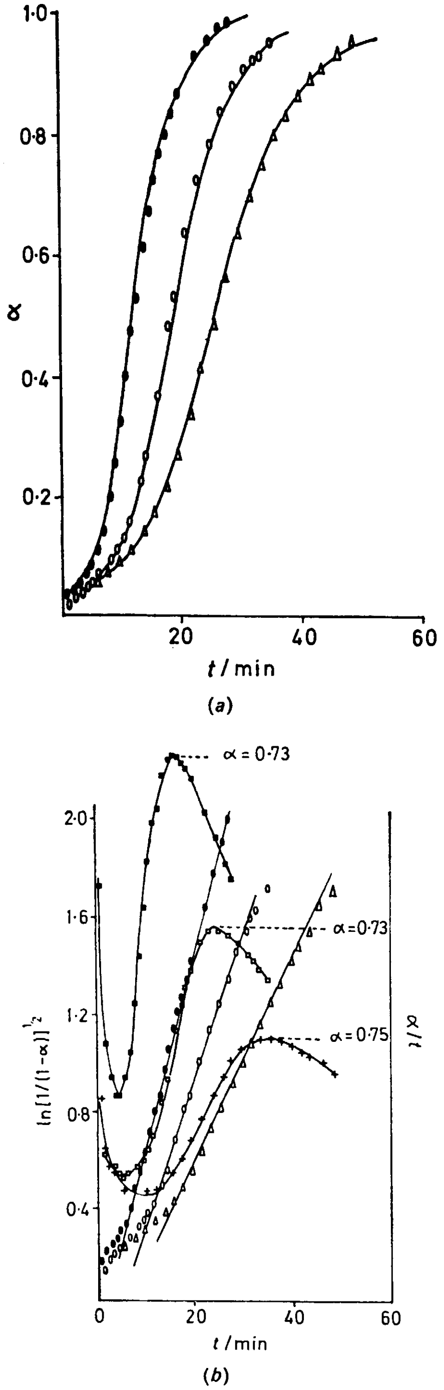

FIGURE 7 (a) Isothermal decomposition curve of $Rb_2[C_2O_4]\cdot H_2O_2$; (b) plot of α/t against t (+, □, ■) and of $\ln[1/(1-\alpha)]^{\frac{1}{2}}$ against t (Avrami–Eroveef kinetics) (△, ○, ●). Temperature = 386 (△,+), 389 (○,□), or 392 K (●,■)

Observations made of the decomposition of single crystals through the optical microscope did not confirm one mechanism rather than the other except that, as in the case of ammonium oxalate hydrate and perhydrate, there was a rapid formation of product on the crystal surfaces which obscured any further observation of the processes involved. This might tend to imply that the contracting-solid type of kinetics (which assumes surface nucleation) would be more suitable.

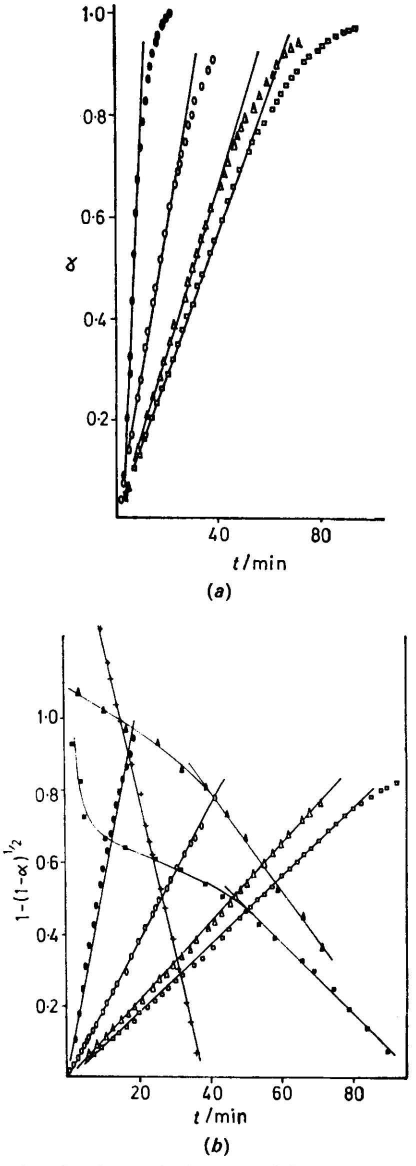

FIGURE 8 (a) Isothermal decomposition curve of $Na_2[C_2O_4]\cdot H_2O_2$; (b) plot of α/t against t (+, ▲, ■) and of $1-(1-\alpha)^{\frac{1}{2}}$ against t (contracting-circle kinetics) (●, ○, △, □). Temperature = 356 (●), 339.5 (○,+), 334 (△,▲), or 330 K (□,■)

$[NH_4]_2[C_2O_4]\cdot H_2O_2$. We were able to get little useful information on the decomposition of this compound. The d.s.c. trace was a mixture of endotherms and exotherms which could not be analysed quantitatively. However, an initial endotherm was found to disappear if the samples were heated at 345 K (*i.e.* above the decomposition temperature of the hydrate) prior to d.s.c. investigation.

Kinetic investigation by t.g.a. was hampered by this partial substitution of H_2O for H_2O_2 in the sample, which ranged from 15% for freshly prepared material to about 30% for samples 12 h after preparation.

Examination of the decomposition of single crystals showed an overall similarity to the observations made on the decomposition of the hydrate. There was a gradual formation of product on the surface, without the nuclei going to discrete sizes, and this obscured further reaction.

Conclusions.—Our results show that the decomposition of the oxalate perhydrates is very similar to that of the corresponding hydrates. The kinetic laws for the processes appear to be the same, and, if the perhydrate decomposes at a temperature sufficiently low to prevent rapid decomposition of H_2O_2, both processes are endothermic. At higher temperatures decomposition of H_2O_2 vapour renders the overall reaction exothermic.

In so far as the inaccuracies of our experiment allow, the heat of a deperhydration is higher than that of the analogous dehydration. Consistent with this observation is the fact that perhydrates decompose at higher temperatures than analogous hydrates, even to the extent that perhydrates of some salts are stable at ambient temperatures, while hydrates are not. It is also noteworthy that hydrogen bonds in perhydrates are shorter (and presumably stronger) than in hydrates.

We also conclude that the analogy between perhydrates and hydrates extends to the mechanism of their decomposition at room temperature. Just as hydrates are in equilibrium with water vapour in the atmosphere, so do perhydrates attempt to maintain equilibrium with H_2O_2 vapour in the atmosphere. That the amount of H_2O_2 in the ambient atmosphere is vanishingly small causes the continuous loss of H_2O_2 even at room temperature.

We thank Dr. R. G. Pritchard for many helpful discussions and Professor J. M. Thomas, F.R.S. for his encouragement.

[9/289 *Received, 23rd February,* 1979]

REFERENCES

[1] C. J. Adams, J. M. Adams, R. G. Pritchard, and V. Ramdas, *J. Inorg. Nuclear Chem.*, 1979, **41**, 937.

[2] T. A. Clarke, Ph.D. Thesis, University College of North Wales, Bangor, 1969; J. M. Thomas and T. A. Clarke, *J. Chem. Soc. (A)*, 1968, 457.

[3] B. F. Pedersen, *Acta Chem. Scand.*, 1964, **18**, 1635.

[4] B. F. Pedersen, *Acta Chem. Scand.*, 1965, **19**, 1815.

[5] B. F. Pedersen, *Acta Chem. Scand.*, 1967, **21**, 779.

[6] J. H. Robertson, *Acta Cryst.*, 1965, **18**, 410.

[7] B. F. Pedersen, *Acta Cryst.*, 1972, **B28**, 746.

[8] B. F. Pedersen and B. Pedersen, *Acta Chem. Scand.*, 1964, **18**, 1454.

[9] B. F. Pedersen, *Acta Chem. Scand.*, 1969, **23**, 1871.

[10] G. G. T. Guarini, R. Spinicci, and D. Donati, *J. Therm. Anal.*, 1974, **6**, 405.

[11] G. G. T. Guarini, R. Spinicci, F. M. Carlini, and D. Donati, *J. Therm. Anal.*, 1973, **5**, 307.

[12] W. E. Garner and L. L. Birkumshaw in ' Chemistry of the Solid State,' ed. W. E. Garner, Butterworths, London, 1955; P. W. M. Jacobs and F. C. Tompkins, *ibid.*; A. K. Galwey and P. W. M. Jacobs, *Proc. Roy. Soc.*, 1960, **A254**, 455.

[13] A. K. Galwey and G. G. T. Guarini, *J.C.S. Chem. Comm.*, 1978, 273.

[14] G. G. T. Guarini and R. Spinicci, *J. Therm. Anal.*, 1972, **4**, 435.

[15] G. G. T. Guarini, R. Spinicci, and D. Donati, Thermal Analysis 1, Proceedings of the Fourth ICTA, Budapest, 1974.

[16] P. A. Giguere, ' Peroxyde D'Hydrogene,' Masson et Cie, Paris, 1975.

[17] T. B. Flanagan, *Trans. Faraday Soc.*, 1961, **57**, 797; *J. Phys. Chem.*, 1962, **66**, 416.